energies

MDPI

Article

Experimental Investigations on Detonation Initiation Characteristics of a Liquid-Fueled Pulse Detonation Combustor at Different Inlet Air Temperatures

Wenhao Tan, Longxi Zheng, Jie Lu *, Lingyi Wang and Daoen Zhou

School of Power and Energy, Northwestern Polytechnical University, Xi'an 710072, China
* Correspondence: lujie@nwpu.edu.cn

Abstract: The detonation initiation characteristics of a single tube liquid-fueled pulse detonation combustor (PDC) is investigated at different inlet air temperatures in this paper. The inner diameter of the PDC is 62 mm. Gasoline and air are used as fuel and oxidant, respectively. The inlet air temperature is 288–523 K and the operating frequency of the PDC is 10~30 Hz. The experimental results show that the deflagration to detonation transition (DDT) distance, detonation initiation time, DDT time and jet ignition time decrease with the increasing operating frequency at the same inlet temperature. When the inlet temperature is 288 K, the DDT distance is shortened from 860.5 mm to 787.7 mm as the operating frequency increases from 10 Hz to 30 Hz. The detonation initiation time, the jet ignition time and the DDT time are reduced from 10.01 ms, 7.66 ms and 2.35 ms to 6.55 ms, 4.99 ms and 1.56 ms, respectively. When the inlet air temperature increases, the atomization and evaporation of the gasoline is improved, which also leads to the decrease in the DDT distance, the detonation initiation time, the jet ignition time and the DDT time. For example, when the inlet air temperature increases from 288 K to 523 K at the frequency of 10 Hz, the DDT distance is shortened from 860.5 mm to 747.2 mm and the detonation initiation time, the jet ignition time and the DDT time is reduced to 5.867 ms, 2.51 ms and 1.11 ms, respectively. Additionally, the self-ignition caused by high inner wall temperature occurs when PDC is operating at high frequency under high inlet air temperature.

Keywords: two-phase detonation; pulse detonation combustor; DDT distance; detonation initiation time; self-ignition

Citation: Tan, W.; Zheng, L.; Lu, J.; Wang, L.; Zhou, D. Experimental Investigations on Detonation Initiation Characteristics of a Liquid-Fueled Pulse Detonation Combustor at Different Inlet Air Temperatures. *Energies* **2022**, *15*, 9102. https://doi.org/10.3390/en15239102

Academic Editor: Adonios Karpetis

Received: 1 November 2022
Accepted: 28 November 2022
Published: 1 December 2022

1. Introduction

Detonation is close to the constant volume combustion process due to the supersonic propagating characteristic of the detonation wave and has the advantage of pressure gain and low entropy generation. These characteristics promise that the detonation-based propulsion systems have theoretically higher thermodynamic efficiency [1,2]. The pulse detonation turbine engine (PDTE) utilizes the pulse detonation combustor (PDC) to replace the traditional combustion chamber in a traditional gas turbine engine, which as a result can change the Brayton cycle in the traditional gas turbine engine to the constant volume cycle and improve the engine performance. The performance calculations show that the PDTE has higher specific thrust and lower specific fuel consumption when compared with traditional gas turbine engines [3–6].

For the pulse detonation turbine engine, detonation initiation of the liquid fuel is crucial for practical application. Generally speaking, the detonation initiation methods can be classified as direct initiation and indirect initiation method. The direct initiation method requires huge energy input so it is impractical in the propulsion system. Therefore, many investigations have been focused on the indirect initiation method of the liquid fuel, which utilizes a small spark to produce an initial flame and initiate the detonation wave through

the deflagration to detonation transition (DDT) process. Sun [6,7] studied the propagation mechanism of the gaseous fuel detonation wave. However, the results [8,9] of the liquid-fueled detonation show that the reaction zone of the liquid-fueled detonation is longer than those of the gaseous detonation and the von Neumann peak can be easily monitored. The detonation wave velocity of the liquid fuel with small droplets is 100–200 m/s lower than the gaseous detonation wave velocity. The velocity deficit can reach as much as 700–800 m/s when the droplets become larger. Wang [10–13] carried out experimental studies on the detonation initiation characteristics of the gasoline/air and kerosene/air mixtures. It was found that with the increasing ignition energy, the detonation initiation time decreased, the DDT distance did not change significantly, and the effect of the ignition energy on the detonation initiation time decreased with the increased operating frequency. In addition, as the diameter of the pulse detonation combustor increased, the detonation initiation time and DDT distance also increased. The operating characteristics of a valveless two-phase PDC under different ignition methods were also discussed. The results showed that the DDT distance was about 150 mm shorter under the pre-detonator initiation method than that under the spark plug ignition method.

The above studies were carried out with the fuel/air mixtures at room temperature. To investigate the temperature effect on the detonation initiation characteristics of different fuel/air mixtures, Schauer [14] conducted detonation initiation tests with the inlet air temperature of 90 °C. Different types of fuel such as propane, aviation gasoline, JP8, and JP10 were injected into the detonation tube at the temperature of 280 °C. It was found that the fuel atomization and mixing process are the key factors to realize detonation initiation under these conditions. Card [15] analyzed the detonation initiation characteristics of the fuel/air mixture by heating the combustible mixture to 300 K, 473 K, and 573 K. The experimental results showed that when the equivalence ratio of the combustible mixture was lower than 1.2, the DDT distance decreased with the increased temperature while the temperature had little effect on the cell size of the JP10/air mixture. The experimental data obtained by Brophy [16] indicated that increasing inlet air temperature could significantly reduce the particle size of JP10 fuel, which would shorten the DDT distance. Akbar [17] conducted experimental measurements of the cell size of the JP10/air mixture under different filling pressure when the JP10 was heated to 135 °C to assist the detonation initiation of the mixture. It was found that the cell size decreased with the increase in the filling pressure. Timothy [18] studied the detonation initiation characteristics of different fuel/air mixtures such as JP8, JP7, JP10, RP1, JP900, and S8 under the supercritical condition. The results showed that with the increase in fuel injection temperature, the DDT time of all the fuel/air mixtures except for the JP10/air mixture was shortened by 15% and the DDT distance was reduced by 30%. Frolov [19,20] successfully initiated the kerosene/air mixture with the help of an air-assist atomizer and the DDT distance was about 2 m. Huang [21] studied detonation initiation characteristics of the kerosene/air mixture in a pulse detonation combustor with an inner diameter of 29 mm under the inlet air temperature of 110 °C. The results indicated that the detonation wave velocity reached 1254.5 m/s and 1191.6 m/s at the operating frequency of 20 Hz and 30 Hz, respectively, and the DDT distance was above 510 mm. Li [22] explored the cold start conditions of jet A-1 fuel by changing the air mass flow rate, the fuel temperature, the fuel droplet size, and the total equivalence ratio. The results showed that the reliability of detonation initiation could be improved by increasing the total equivalence ratio. The research results of Li and Xu [23,24] showed that the increase in incoming air temperature was beneficial to the detonation initiation of kerosene and air mixture, but the structure of the inlet aero-valve affects the success rate of ignition and detonation initiation. The numerical calculation results of Nguyen [25] showed that the mass fraction of fuel in the evaporative state directly affected the successful detonation initiation of a liquid-fueled pulse detonation combustor. No matter whether the droplet in the pulse detonation combustor is completely evaporated or not, it cannot be initiated if the fuel vapor ratio is too high or too low (in this study, the

equivalence ratio is 0.7–2.35). When the fuel is not fully evaporated, the wave velocity is lower than that of complete evaporation.

The above studies reveal the detonation initiation characteristics of liquid-fueled pulse detonation combustor at different inlet air temperatures or with heated fuel. Moreover, the detonation initiation characteristics of liquid-fueled pulse detonation combustor were mainly obtained by multi-cycle experiment under room temperature air or single-cycle experiment of heated air. There are no systematic studies on multi-cycle pulse detonation initiation characteristics under different inlet air temperatures. The PDC is operated at the downstream of the compressor in the PDTE. The inlet air of the PDC is compressed by the compressor and its temperature is raised. For example, when the compressor pressure ratio is seven, the inlet air temperature of the PDC is about 532 K. Therefore, the detonation initiation characteristics of the liquid-fueled pulse detonation combustor at different inlet air temperatures need to be systematically discussed.

In this paper, a liquid-fueled PDC with an inner diameter of 62 mm was set up and tested under different inlet air temperatures from 288 K to 523 K at operating frequencies of 10–30 Hz. The detonation initiation characteristics of the PDC were revealed under these conditions. Furthermore, the self-ignition phenomenon observed by PDC under some working conditions is discussed. The present studies offer some experience to design the PDC and provide some theoretical and experimental bases to impel the application of the pulse detonation turbine engine.

2. Experimental Setup

Figure 1a shows the schematic diagram of the experimental system. The whole system is composed of an air supply system, an air heater, a fuel supply system, an ignition system, a single-tube PDC, and a data acquisition system.

The power of the air heater is 180 KW, which can heat the inlet flow from room temperature to 600 K. The valveless PDC consists of a mixing section, an ignition section, a detonation tube and a convergent nozzle. The inner diameter of all the sections is 62 mm. The total length of the mixing section and the ignition section is 200 mm. An intake cone is welded in the middle of the mixing section using two supports. The end side of the cone partially closes the flow field and acts as a thrust wall. Gasoline is fed into the mixing section through a fuel pipe. A twin-fluid air-assist atomizer is used for gasoline injection. The length of the detonation tube is 933 mm. Shchelkin spiral structure with a pitch of 60 mm is set in the detonation tube to promote the deflagration to the detonation transition process. The exit diameter of the convergent nozzle is 40 mm to simulate the throat of the downstream turbine guide. A picture of the air heater and the PDC is shown in Figure 1b.

A hot jet ignition method is used to ignite the initial flame. The schematic structure of the hot jet ignition system is shown in Figure 1c. The hot jet ignition system is ignited by the spark plug and the ignition energy is less than 150 mJ. Gasoline and air are used as fuel and oxidant respectively. The valveless method is adopted to control the supply of gasoline and air.

A gas turbine flow meter is installed in the PDC air supply system to measure the mass flow rate of the air (w_a) entering into the PDC, and a gear flow meter is used in the fuel supply system to measure the fuel flow rate (w_f). A T-type thermocouple (T_t) is installed at the inlet of the mixing section to measure the inlet flow temperature. A piezoresistive sensor (Pf) is installed on the fuel pipe of the fuel supply system to measure the fuel supply pressure. A piezoresistive sensor is installed at point 0 to measure the pressure in the mixing section. To monitor the dynamic pressure and flame velocity in the PDC, a set of sensor mounting seats 1–7 are fabricated on the detonation tube. Pressure sensors or ion probes can be installed. The distances between each sensor mounting seat and the ignition position are 98, 300, 437, 585, 680, 788 and 883 mm, respectively. Furthermore, a water cooling system is designed to avoid measurement errors or even failure of the pressure sensors caused by the high temperature. In the tests, piezoelectric sensors (SINOCERA CYD-205, measuring range: 0–10 MPa, frequency response: 500 KHz, measurement error:

±72.5 mV/MPa) are used to measure the pressure along the detonation tube (*P*1–*P*7). The flame velocity is recorded by the ion probes (*I*1–*I*7). All the dynamic data are monitored and collected through the DEWE3020 high-speed data acquisition system with a total of 16 channels, and the sampling rate was 200 K samples/s.

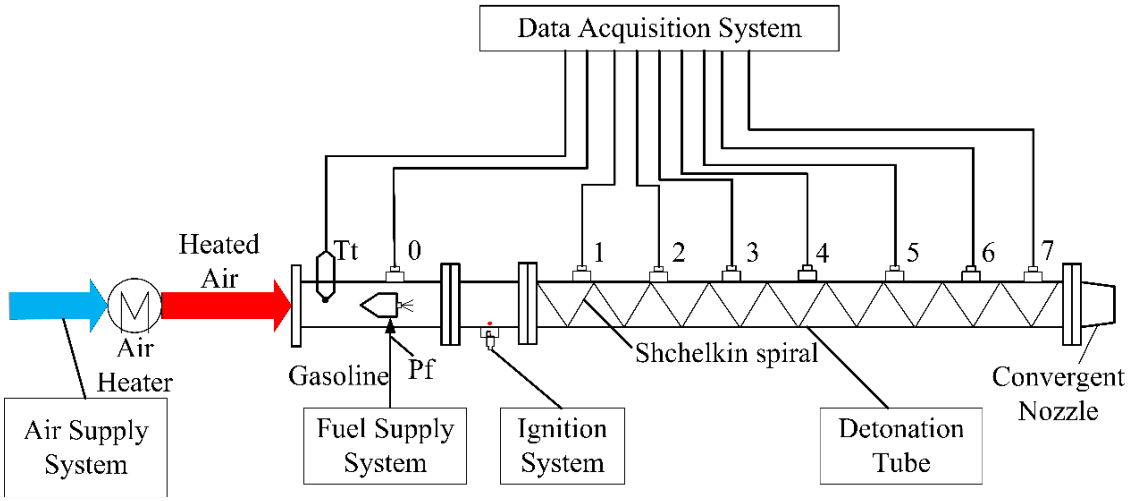

(**a**)

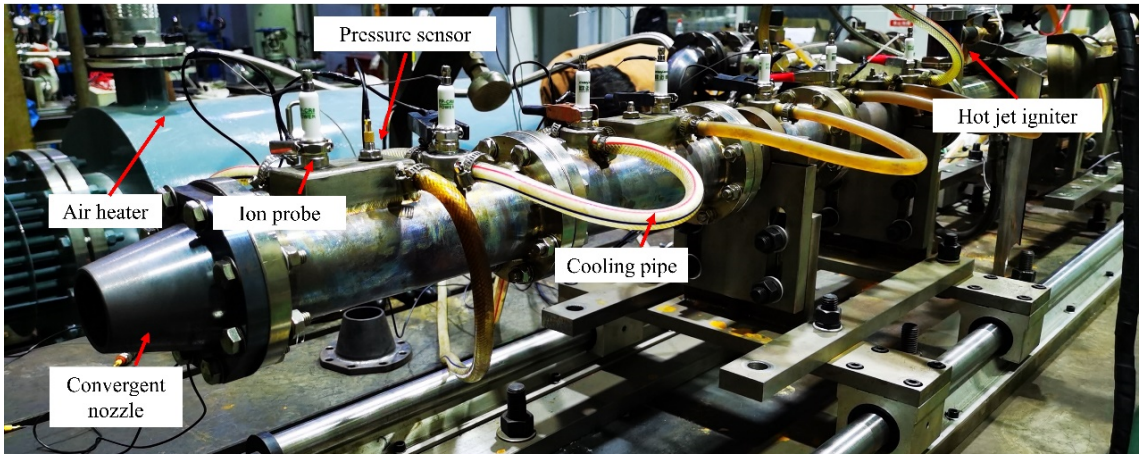

(**b**)

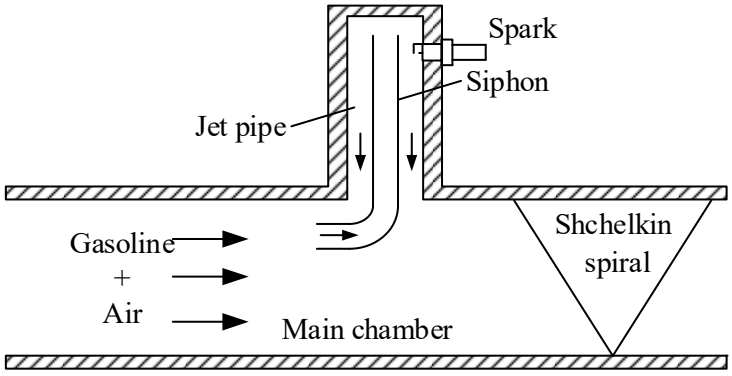

(**c**)

Figure 1. Schematic diagram of the PDC experimental system. (**a**) Schematic diagram of the valveless two-phase PDC test system. (**b**) The valveless two-phase PDC test system. (**c**) Hot jet igniter.

3. Results and Analysis

In this paper, the multi-cycle operation of the PDC was carried out under different inlet air temperatures (288 K, 323 K, 373 K, 423 K, 473 K, and 523 K) at the frequency of 10–30 Hz. The experimental conditions and the air velocity in PDC under different working conditions are shown in Tables 1 and 2. According to the air velocity in PDC in Table 2, it can be judged that the pulse detonation chamber is overfilled under all the operating conditions. In addition, each test for one specific condition is repeated three times to reproduce the phenomenon.

Table 1. Airflow and fuel flow in PDC at different operating frequencies.

f (Hz)	w_a (kg/h)	w_f (mL/s)
10	277.83	7.0
15	416.75	10.5
20	535.82	13.6
25	674.73	17.1
30	892.17	22.6

Table 2. Air velocity in PDC at different working conditions.

f (Hz)	10	15	20	25	30
Air velocity in PDC when T_t = 288 K (m/s)	15.03	21.52	27.41	32.78	337.68
Air velocity in PDC when T_t = 323 K (m/s)	16.77	23.94	30.42	36.31	41.64
Air velocity in PDC when T_t = 373 K (m/s)	19.21	27.33	34.64	41.19	47.14
Air velocity in PDC when T_t = 423 K (m/s)	21.64	30.7	38.79	46.00	54.49
Air velocity in PDC when T_t = 473 K (m/s)	24.04	33.99	42.84	50.69	57.69
Air velocity in PDC when T_t = 523 K (m/s)	26.42	37.26	46.81	55.29	62.77

The experimental results are divided into four sections. Firstly, the operability of the PDC under different conditions is discussed. Then, the pressure propagation characteristic along the tube is revealed. Furthermore, the detonation initiation characteristics such as the DDT distance, the detonation initiation time, the jet ignition time and the DDT time are analyzed under different inlet air temperatures at the frequency ranges of 10–30 Hz. Additionally, the self-ignition caused by high inner wall temperature when PDC is operating at high frequency under high inlet air temperature is discussed.

Since the spark plug produces strong electromagnetic interference during the discharging process, the ignition starting time can be determined according to the ignition noise on the pressure profiles monitored by the data acquisition system. After the ignition time is determined, the pressure propagation time t_{pressure} and flame propagation time t_{flame} of each measuring point can be calculated. If t_{pressure} equals t_{flame}, the pressure wave is coupled with the combustion wave, which means the detonation wave is formed; then, the detonation initiation time and the DDT distance could be determined. In the experiment, the velocity of the combustion wave is calculated by $\Delta x/\Delta t$ (Δx is the distance between two ion probes and Δt is the time difference between two adjacent ion probes).

3.1. Operational Characteristics of the PDC under Different Inlet Air Temperature

The stability of multi-cycle PDC under different working conditions is the premise of engineering application. Due to the different inlet air temperatures, the fuel atomization and mixing process are also different which may affect the ignition reliability and detonation initiation characteristics of the PDC. Figure 2 shows the pressure waveform within 1 s at measuring point 7 under the inlet air temperature from 288 K to 523 K at the frequency of 10–30 Hz. It can be seen that the PDC can operate stably under all working conditions except if the inlet air temperature is 523 K and the operating frequency is 30 Hz. Moreover, the unstable operation of this working condition is affected by self-ignition which will be analyzed later.

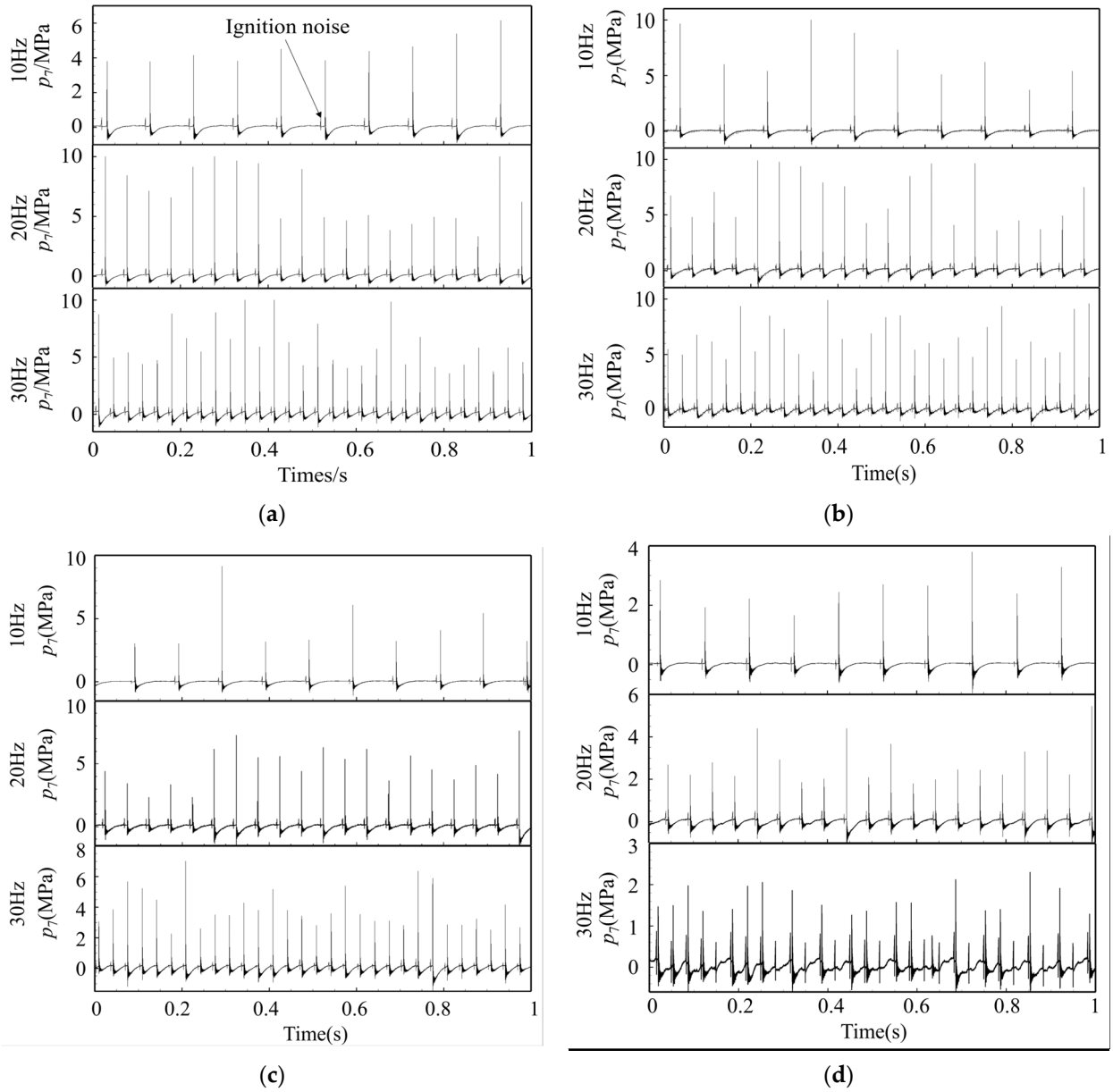

Figure 2. Pressure history at different working conditions. (**a**) Pressure profiles at 10–30 Hz when T_t = 288 K. (**b**) Pressure profiles at 10–30 Hz when T_t = 323 K. (**c**) Pressure profiles at 10–30 Hz when T_t = 423 K. (**d**) Pressure profiles at 10–30 Hz when T_t = 523 K.

As shown in Figure 2b, the peak pressure of P7 with the operating frequency of 10 Hz is greater than the C-J pressure when the inlet air temperature is 288 K. However, it cannot be judged that detonation waves have been formed under all working conditions. This is because the theoretical C-J also changes with the change in inlet air temperature. The forming of gaseous detonation can generally be determined by the detonation wave velocity, the peak pressure, and the rise time of the peak pressure. However, the velocity of the two-phase detonation is usually lower than the C-J velocity due to the wall losses, incomplete combustion of the liquid fuel before the C-J plane, and the energy loss due to back-propagating waves. Therefore, the peak pressure is regarded as the main criterion for judging the forming of the two-phase detonation. The wave velocity of the two-phase detonation measured in the experiment can be used as a reference for whether the detonation is obtained. It is generally considered that the combustion wave velocity of two-phase detonation needs to achieve at least 70% of the C-J velocity [26,27].

Figure 3 shows the average peak pressure from P1 under different working conditions. The theoretical C-J pressure under different working conditions calculated by Chemical Equilibrium and Applications (CEA) code is shown in Figure 3. As shown in Figure 3a, the peak pressure at P7 is higher than C-J pressure at each incoming temperature under the operating frequency of 10 Hz. However, when the inlet air temperature is lower than 373 K, P6 is lower than C-J pressure. As the inlet air temperature increases to 373 K or higher, the peak pressure at P6 increases and is greater than the C-J pressure. When the operating frequency of PDC is 15 Hz (Figure 3b), the pressure variation trend of P6 and P7 is similar to that of 10 Hz, and a higher pressure peak is formed at P5 than P6 at the downstream temperatures of 473 K and 523 K, indicating that an overdriven detonation wave is formed near P5. For the operating frequencies of 20 Hz, 25 Hz and 30 Hz, the formation of an overdrive detonation wave is also detected at P4 or P5, the peak pressure of the overdrive detonation wave is greater when the inlet air temperature is the same and the operating frequency is increased. Further, under these three operating frequencies, the peak pressure of P5–P7 is greater than the C-J pressure. However, whether to form a fully developed detonation wave needs to be discussed in combination with wave velocity.

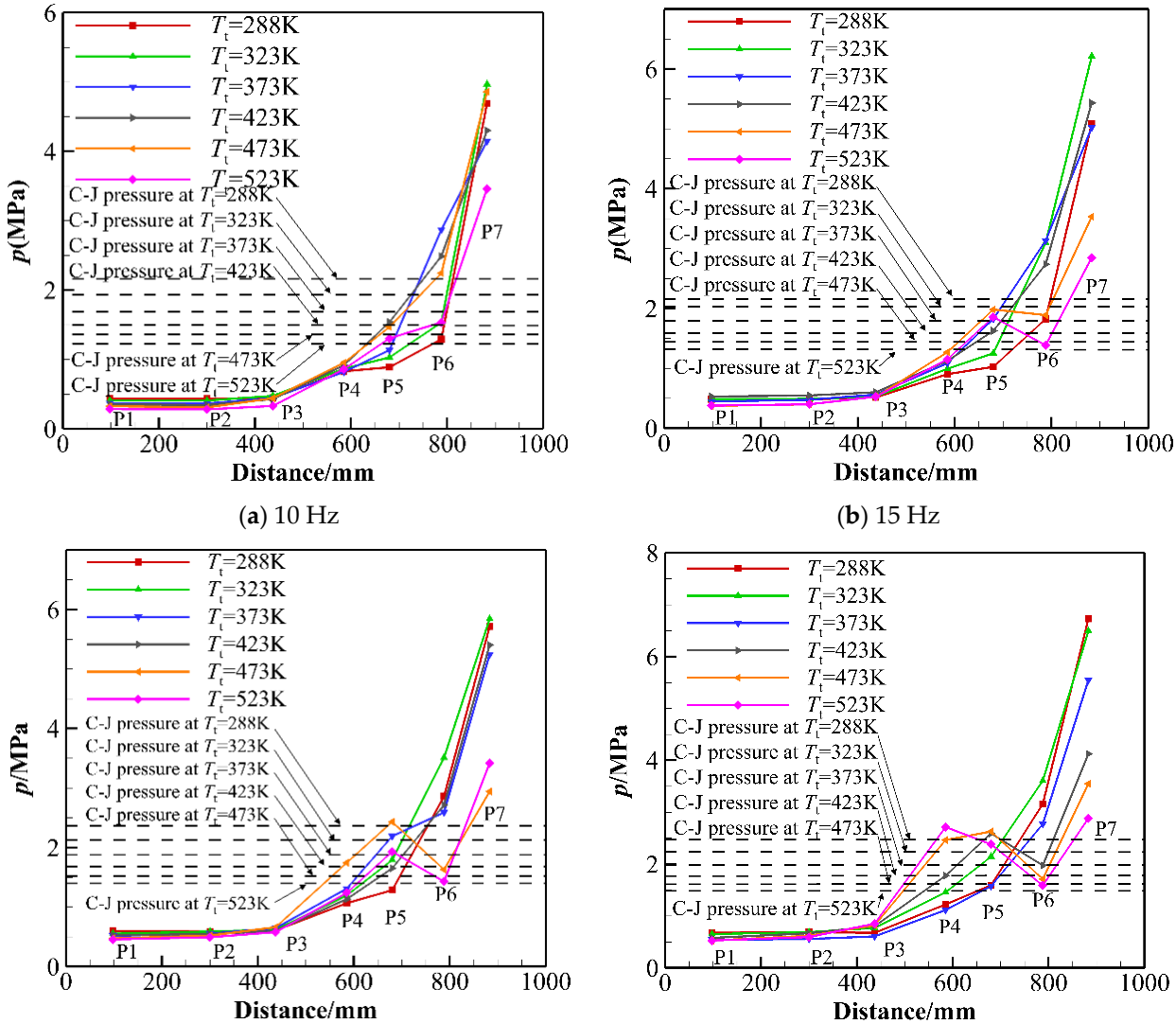

(**a**) 10 Hz

(**b**) 15 Hz

(**c**) 20 Hz

(**d**) 25 Hz

Figure 3. *Cont.*

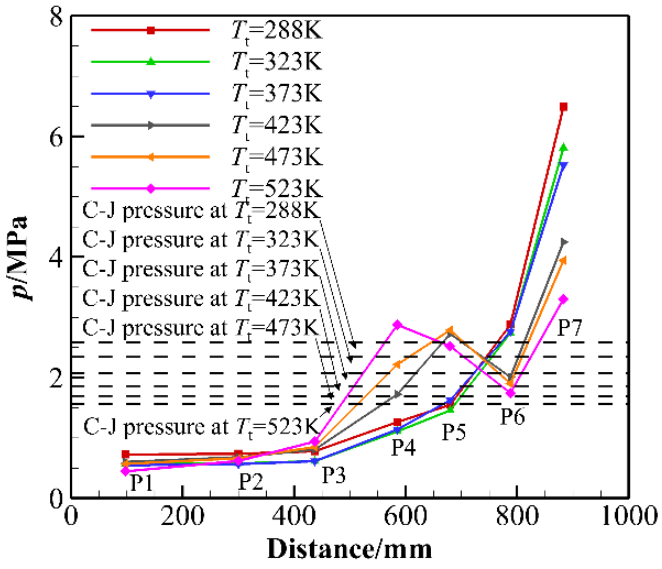

(**e**) 30 Hz

Figure 3. Average peak pressure under different working conditions.

Figure 4 presents the averaged flame propagation velocity $V_{I5–I6}$ and $V_{I6–I7}$ at different conditions based on the signal of the ion probes. $V_{I5–I6}$ and $V_{I6–I7}$ indicate the averaged velocity of the measuring point 5 to point 6 and the measuring point 6 to point 7, respectively. The data in Figure 4 shows that when the inlet air temperature is 288 K, $V_{I6–I7}$ is greater than 70% of the C-J velocity only when the operating frequency is 30 Hz. However, $V_{I5–I6}$ is greater than 70% of the C-J velocity under other working conditions. Combined with the peak pressure in Figure 3 and the combustion wave velocity data in Figure 4, it can be judged that the fully developed detonation wave has been obtained under other working conditions except the inlet air temperature is 288 K and the operating frequency range is 10–25 Hz. Even though the peak pressure measured by *P*7 is greater than the C-J pressure at the temperature of 288 K when the frequency is 10–25 Hz, the averaged flame propagation velocity $V_{I5–I6}$ and $V_{I6–I7}$ are between 800 m/s and 1200 m/s, which are lower than 70% of the C-J velocity. Since the accurate wave velocity along the detonation tube cannot be measured, it is impossible to judge whether the fully developed detonation waves are formed under this condition. In addition, the averaged flame propagation velocity $V_{I5–I6}$ in Figure 4a decreases suddenly in the operation frequency of 25 Hz. This is because when the intake air temperature is 288 K and the frequency is lower than 25 Hz, the explosion in PDC caused by the greater non-uniformity of the fuel distribution may cause a higher flame speed in the experiment.

Figure 5a shows the enlargement of the pressure profile and the ion probe signal at measuring point 7 with the inlet air temperature of 288 K at the frequency of 30 Hz. The pressure propagation time t_{pressure} and the flame propagation time t_{flame} at measuring point 7 could be calculated. t_{pressure} is the time required from the ignition of the spark plug to the moment when the pressure at the measuring point rises to 10% of the peak pressure. t_{flame} is the time required from the ignition of the spark plug to the rising edge of the ion signal at the measuring point. If the t_{pressure} equals t_{flame}, the shock wave is consistent with the combustion wave, which means the detonation wave is formed. To determine the formation of detonation wave under inlet air temperature of 288 K, the pressure propagation time and flame propagation time of each measuring point are calculated at the frequency range from 10 Hz to 30 Hz, which are presented in Figure 5b,c. It shows that the pressure waves and the flame front are separated before measuring point 6. The flame front is coupled with the pressure wave at measuring point 7, indicating that the detonation wave is formed. However, since the detonation initiation position is close to the outlet of the detonation tube, the average flame velocity of $V_{I5–I6}$ and $V_{I6–I7}$ are a little low-lying. In a word, it can

be concluded that the detonation wave is formed under all the inlet air conditions at the frequency of 10 Hz to 30 Hz.

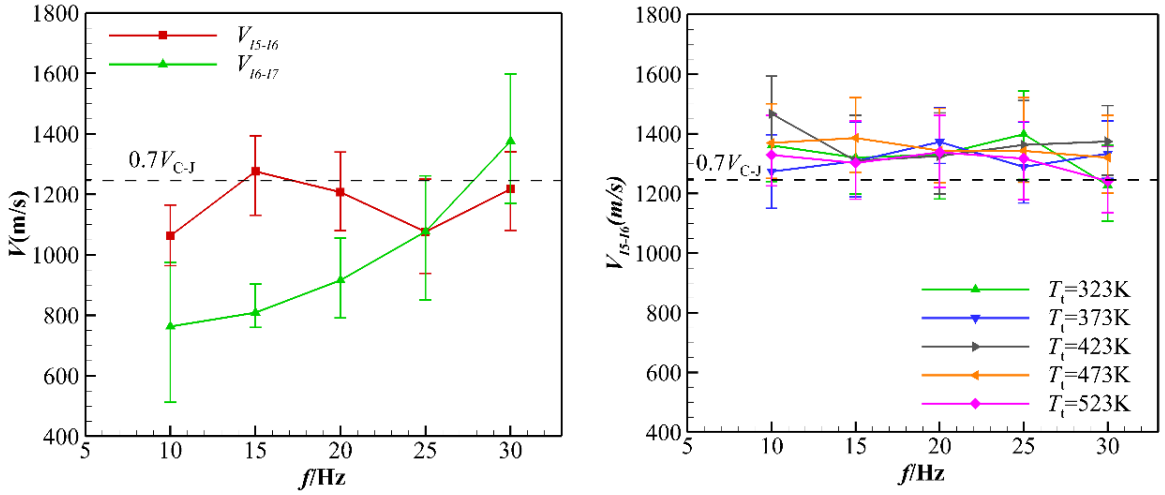

(**a**) *T*t = 288 K (**b**) *T*t = 323–523 K

Figure 4. Flame propagation velocity in PDC measuring point 5~6 and measuring point 6~7 at different working conditions.

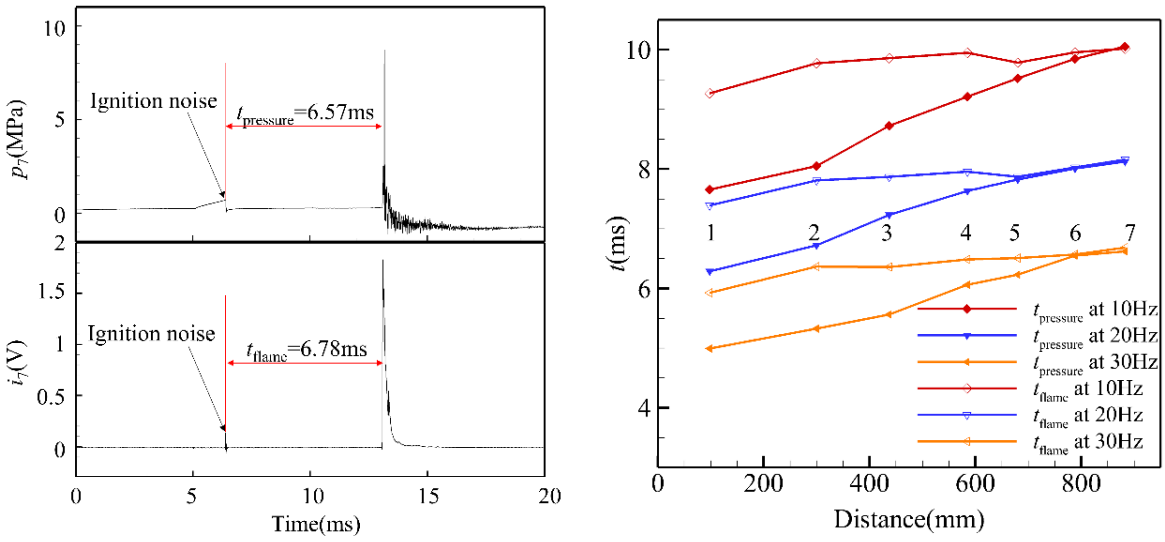

(**a**) (**b**)

Figure 5. *Cont.*

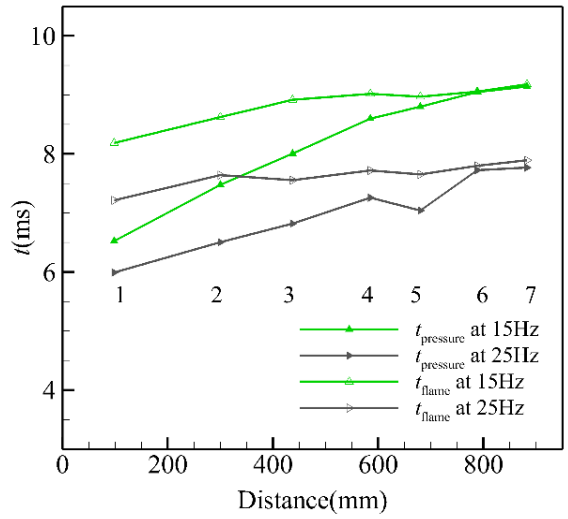

(**c**)

Figure 5. $t_{pressure}$ and t_{flame} at each measuring point of PDC when T_t = 288 K. (**a**) $t_{pressure}$ and t_{flame} at measuring point 7 when f = 30 Hz. (**b**) $t_{pressure}$ and t_{flame} at 10 Hz, 20 Hz, 30 Hz. (**c**) $t_{pressure}$ and t_{flame} at 15 Hz, 25 Hz.

3.2. Characteristics of the DDT Distance

The DDT distance of the PDC under different operating conditions is calculated by the flame propagation time and the pressure propagation time, which are shown in Figure 6.

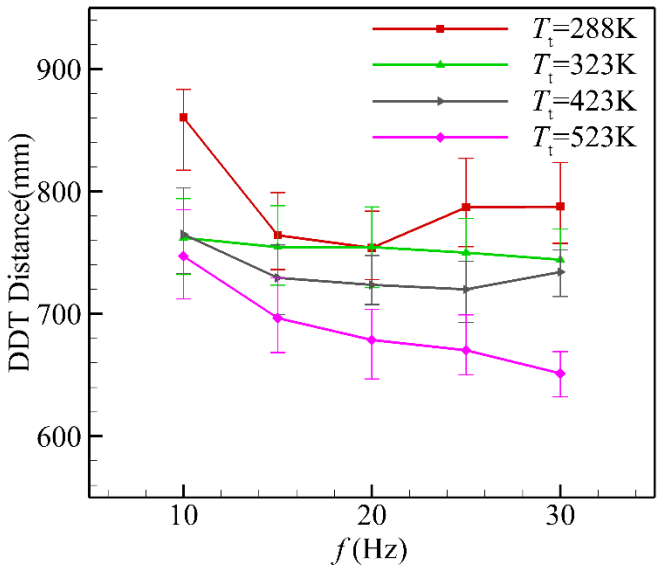

Figure 6. The DDT distance of PDC at different working conditions.

Figure 6 shows that the DDT distance decreases with the increase in the inlet air temperature at the same operating frequency. For example, the DDT distance is shortened from 860.5 mm to 747.2 mm when the inlet air temperature is increased from 288 K to 523 K under 10 Hz. The DDT distance is shortened from 787.7 mm to 651.4 mm when the inlet air temperature is increased from 288 k to 523 K under 30 Hz. There are two main reasons. The first one is that with the increase in inlet air temperature, the atomization and evaporation process of fuel droplets in the detonation tube accelerate, which is beneficial to the initiation of the detonation wave. Another factor is that the inlet air is used as atomizing air of the twin-fluid air assist atomizer in this experiment. As the inlet air temperature increases, the

atomization air temperature also increases, which also improves the atomization of the liquid fuel [28].

In addition, the DDT distance also tends to decrease with the increase in the operating frequency at the same inlet air temperature. For example, when the inlet flow temperature is 288 K, the DDT distance is shortened from 860.5 mm to 787.7 mm as the operating frequency is increased from 10 Hz to 30 Hz. When the operating frequency increases, the total pressure of the inlet air increases, which means the atomization pressure of the twin-fluid air-assist atomizer also increases since the atomization air is introduced from the inlet of the PDC. Therefore, the atomization of the liquid fuel is be improved, which is beneficial to the initiation of the detonation wave. In addition, with the increase in operating frequency, the wall temperature of the detonation chamber also increases [29]. The heat exchange between the fresh mixtures and the wall during the filling process also speeds up the evaporation and the mixing of the fuel and the oxidant, which catalyzes the generation of the detonation wave.

3.3. Characteristics of the Detonation Initiation Time

The detonation initiation time, the jet ignition time and the DDT time are also important characteristics of the PDC. Figure 7 provides a schematic definition of these parameters. The detonation initiation time $t_{ig\text{-}det}$ is the time interval from the time of ignition to the time of detonation initiation. The jet ignition time t_{jet} is the time interval from the time of ignition to the time when the pressure rise is 10% above the baseline pressure at the measuring point closest to the ignition position. The DDT time t_{DDT} is the time interval for the deflagration to the detonation transition process, where $t_{ig\text{-}det} = t_{jet} + t_{DDT}$.

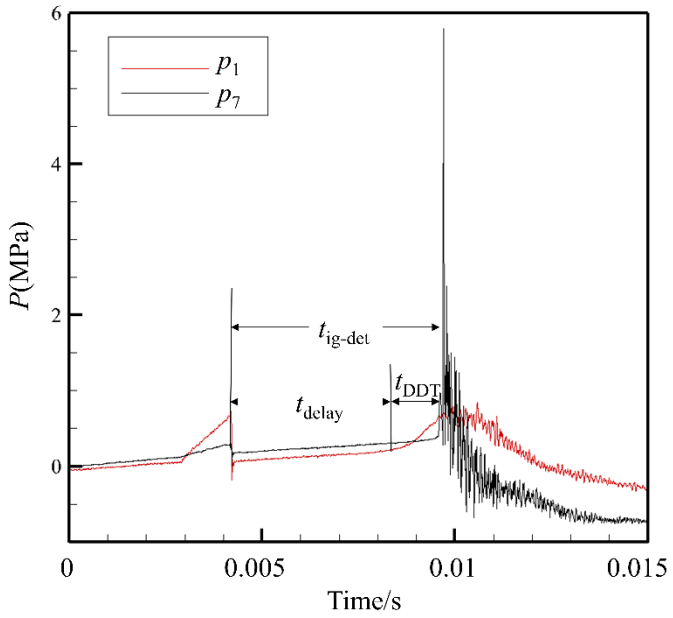

Figure 7. Schematic of the definition of detonation initiation time, jet ignition time and DDT time.

Figure 8 shows the variation of the detonation initiation time, the jet ignition time and the DDT time as the operating frequency increased from 10 Hz to 30 Hz under different inlet air temperatures. The detonation initiation time $t_{ig\text{-}det}$ of the PDC is between 3 and 10 ms, and the jet ignition time accounts for 64–77% of the detonation initiation time. Due to the hot jet igniter adopted in the experiment, the jet ignition time includes the propagation time of the initial flame in the ignition chamber and the time of the flame propagating to measuring point 1. Due to the slow propagation speed of the initial flame, the jet ignition time accounts for a large proportion of the detonation initiation time.

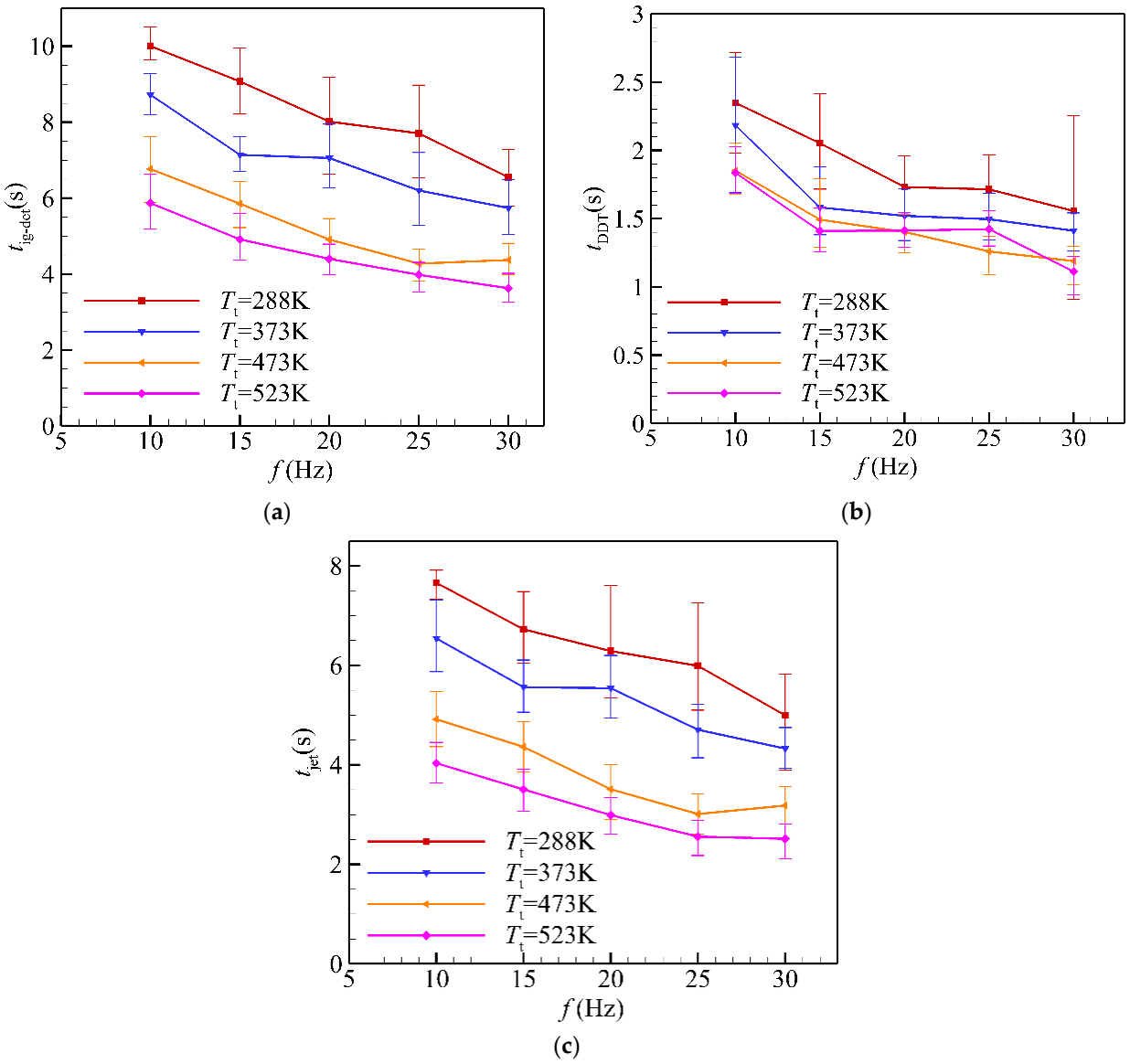

Figure 8. Detonation initiation time, jet ignition time and DDT time at different working conditions. (**a**) The detonation initiation time of PDC. (**b**) The DDT time of PDC. (**c**) The jet ignition time of PDC.

In addition, the data in Figure 8 proves that the detonation initiation time, jet ignition time and DDT time decreased with the increased frequency when the inlet air temperature stayed the same. For example, when the inlet air temperature is 288 K, as the operating frequency of the PDC is increased from 10 Hz to 30 Hz, the detonation initiation time is reduced from 10.01 ms to 6.55 ms, the DDT time is reduced from 2.35 ms to 1.56 ms, and the jet ignition time is reduced from 7.66 ms to 4.99 ms. When the operating frequency is the same, the detonation initiation time, the jet ignition time, and the DDT time would decrease with the increased inlet air temperature. For example, when the operating frequency is 10 Hz, as the inlet air temperature increases from 288 K to 523 K, the detonation initiation time is decreased from 10.01 ms to 5.867 ms, the jet ignition time is decreased from 4.99 ms to 2.51 ms, and the DDT time is decreased from 1.56 ms to 1.11 ms. The reason is mainly the improved atomization and evaporation of the liquid fuel in the PDC as the inlet air temperature or operating frequency increases.

3.4. Self-Ignition Phenomenon Analysis

The self-ignition phenomenon is observed when PDC is operating with high frequency under the high inlet air temperature. Figure 9 shows the pressure waveforms of P1, P3 and P7 at the incoming temperature of 523 K and the frequency of 30 Hz. Generally speaking, the spark plug ignites the combustible mixture, and then the initial flame propagates along the detonation chamber and generates a fully developed detonation wave through the DDT process. In this case, the pressure peak obtained by each sensor is located after the ignition noise. However, in Figure 8a, there is a pressure pulsation in front of the ignition noise, which indicates that the combustible mixture in the detonation chamber has self-ignition before the ignition of the spark plug, and the pressure peak is low because the detonation chamber is not fully filled when self-ignition occurs. In Figure 9a, there is a self-ignition during one working cycle, and the combustible mixture is not purged in time, which leads to the ignition failure of the next working cycle. If self-ignition occurs several times in one cycle of PDC (Figure 9b), the PDC does not work stably for several cycles.

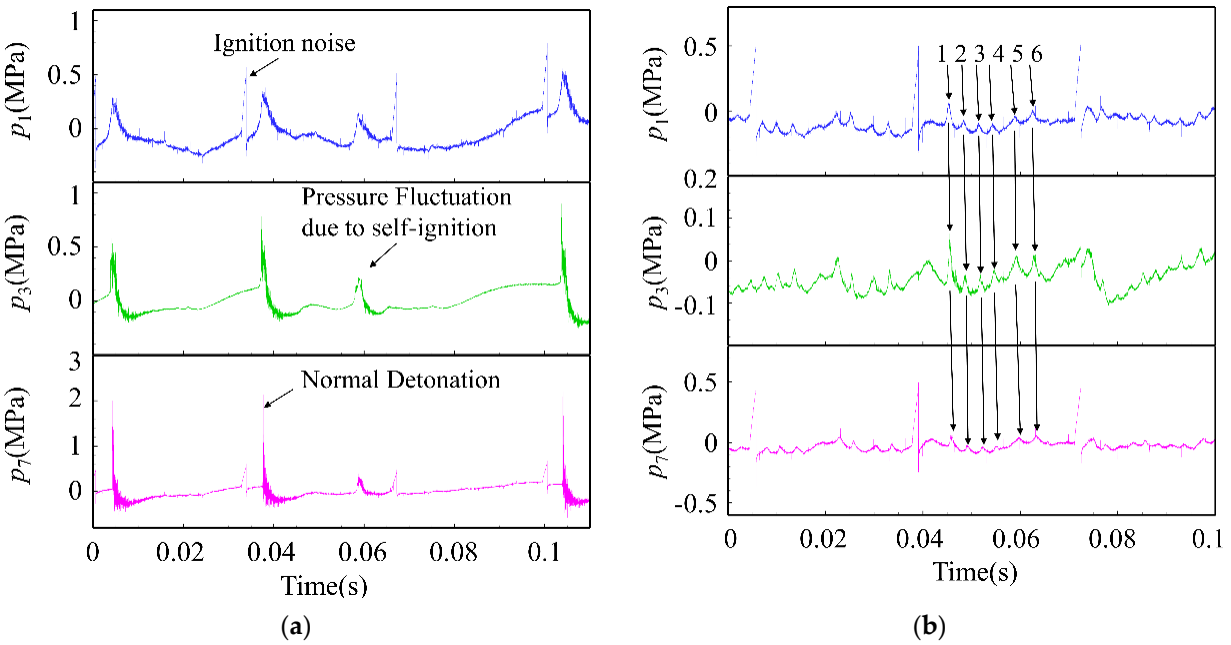

Figure 9. Self-ignition phenomenon with the frequency of 30 Hz under T_t = 523 K. (**a**) Self-ignition phenomenon 1. (**b**) Self-ignition phenomenon 2.

Since the experimental research is aimed at the multi-cycle PDC, the self-ignition may be due to the incomplete purging of the burned mixture in the PDC, and the fresh combustible mixture is ignited after contact with high-temperature combustion products. It may also be the case that because the wall temperature in the PDC is too high and exceeds the burning point of the fuel, the filled fresh combustible mixture is ignited. Table 3 shows the time from ignition to the first self-ignition in the experiment. It can be seen that self-ignition occurs at high temperatures and high frequencies. Therefore, combined with the pressure data in Figure 2, the self-ignition may be caused by the excessive wall temperature in the PDC. It is worth mentioning that although self-ignition does not occur under other working conditions, it does not mean that self-ignition will not occur under these working conditions. This is because each operation time in the experiment lasts about 40 s, and the wall temperature of the PDC does not reach the thermal balance. If the ignition time is longer, self-ignition may also occur.

Table 3. Self-ignition time at different working conditions.

f (Hz)	10	15	20	25	30
Self-ignition time when T_t = 288 K (s)	/	/	/	/	/
Self-ignition time when T_t = 323 K (s)	/	/	/	/	/
Self-ignition time when T_t = 373 K (s)	/	/	/	/	/
Self-ignition time when T_t = 423 K (s)	/	/	/	12.91	5.39
Self-ignition time when T_t = 473 K (s)	/	/	1.669	2.467	2.727
Self-ignition time when T_t = 523 K (s)	/	/	1.121	0.715	0.3

To find out the location of self-ignition, Figure 10 shows the pressure waveform of self-ignition at each measuring point in Figure 9. According to the results in Figure 10, no matter whether it is a single self-ignition or multiple self-ignitions occurring in one cycle, the pressure disturbance propagates from P1 to P7 in turn, which is enough to indicate that the location of self-ignition should be in front of the detonation tube, that is, the self-ignition flame would be formed in the mixing section and ignition section. However, it cannot be determined whether self-ignition occurred in the mixing section or ignition section through current experimental data. Since self-ignition triggers detonation failure or even unstable operation of the PDC, further research is necessary to determine the location of self-ignition, and cooling technology should be used in future applications to avoid self-ignition.

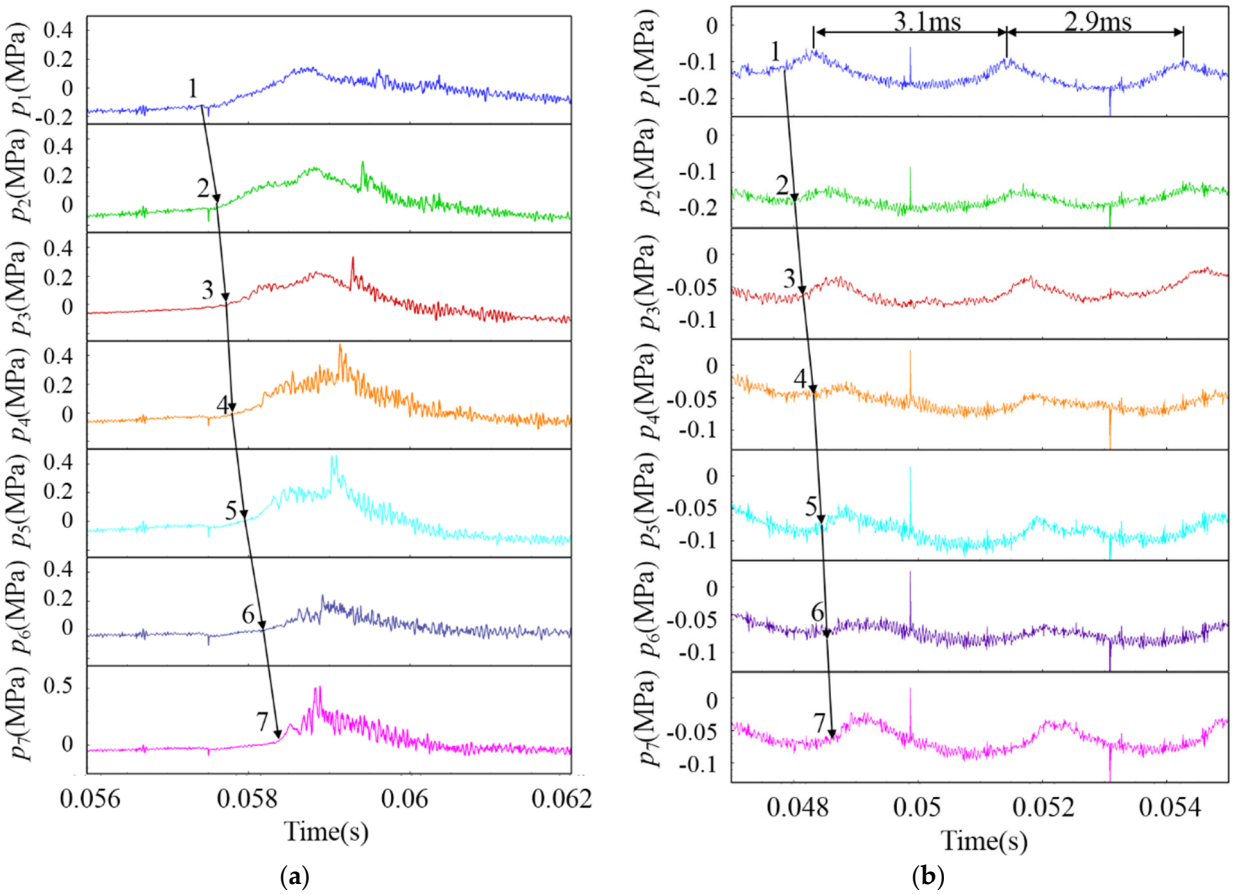

Figure 10. Enlarged pressure waveform caused by self-ignition in Figure 9. (**a**) Enlarged view of Figure 9a. (**b**) Enlarged view of Figure 9b.

4. Conclusions

(1) In this paper, the multi-cycle detonation initiation characteristics of a liquid-fueled pulse detonation combustor at different inlet air temperatures are experimentally studied. The operability of the PDC under different inlet air temperatures at the frequency range of 10 Hz to 30 Hz is proved.

(2) The detonation initiation characteristics such as the DDT distance and the DDT time are obtained under inlet air temperature from 288 K to 523 K at the frequency of 10 Hz to 30 Hz. The results show that fully developed detonation waves have been obtained under all the tests according to the peak pressure and flame velocity at the measuring points near the end of the detonation chamber.

(3) The detonation initiation time of the PDC is within 3–10 ms and the jet ignition time accounts for 64–77% of the detonation initiation time under all the tests. The DDT distance, the detonation initiation time, the DDT time, and the jet ignition time all reduce with the increasing frequency at the same temperature. For example, when the inlet flow temperature is 288 K, the DDT distance is shortened from 860.5 mm to 787.7 mm with the frequency increased from 10 Hz to 30 Hz. The detonation initiation time, the jet ignition time, and the DDT time reduce from 10.01 ms, 7.66 ms and 2.35 ms to 6.55 ms, 4.99 ms and 1.56 ms, respectively. The inlet air temperature also speed up the DDT process due to the improved atomization and evaporation process under higher inlet air temperatures. The DDT distance is shortened as the inlet air temperature increases from 288 K to 523 K. The detonation initiation time, the jet ignition time and the DDT time also reduce. When the operating frequency is 10 Hz, the DDT distance is shortened to 747.2 mm with the inlet air temperature increased from 288 K to 523 K. The DDT time is shortened to 5.867 ms, 2.51 ms and 1.11 ms, respectively.

(4) The self-ignition phenomenon is observed when PDC is operating at high frequency under high inlet air temperature, which leads to detonation failure or unstable operation of the PDC. The reason for this phenomenon may be the inner wall temperature of the mixing section or ignition section being too high, which ignites the combustible mixture. Therefore, it is necessary to optimize the fuel mixing and ignition structure and equip it with cooling technology to ensure the stable operation of the PDC. The research results of this paper point out the operating characteristics of the PDC at different inlet temperatures, including detonation initiation and self-ignition, which provides a reference for the engineering application design of PDC in the future and is conducive to promoting the engineering application of pulse detonation turbine engine.

Author Contributions: Methodology, W.T. and L.Z.; Validation, W.T.; Formal analysis, W.T.; Investigation, W.T., L.W. and D.Z.; Data curation, W.T.; Writing—original draft, W.T.; Writing—review & editing, J.L. All authors have read and agreed to the published version of the manuscript.

Funding: This research received no external funding.

Conflicts of Interest: The authors declare no conflict of interest.

References

1. Wintenberger, E.; Shepherd, J. Stagnation hugoniot analysis for steady combustion waves in propulsion system. *J. Propul. Power* **2006**, *22*, 835–844. [CrossRef]
2. Roy, G.D.; Frolov, S.M.; Borisov, A.M.; Netzer, D.W. Pulse detonation propulsion: Challenges, current status and future perspective. *Prog. Energy Combust. Sci.* **2004**, *30*, 545–672. [CrossRef]
3. Li, X.F.; Zheng, L.X.; Qiu, H.; Chen, J. Experimental investigations on the power extraction of a turbine driven by a pulse detonation combustor. *Chin. J. Aeronaut.* **2013**, *26*, 1353–1359. [CrossRef]
4. Ionio, Q.A.; Paul, I.K. Evaluation of a high bypass turbofan hybrid utilizing a pulsed detonation combustor. In Proceedings of the 43rd AIAA/ASME/SAE/ASEE Joint Propulsion Conference & Exhibit, Cincinnati, OH, USA, 8–11 July 2007.
5. Qiu, H.; Xiong, C.; Yan, C.J. Propulsive performance of ideal detonation turbine based combined cycle engine. *J. Eng. Gas Turbines Power* **2012**, *134*, 081201. [CrossRef]

6. Dean, P.P.; James, L.F. Engine system performance of pulse detonation concepts using the NPSS Program. In Proceedings of the 38th AIAA/ASME/SAE/ASEE Joint Propulsion Conference & Exhibit, Indianapolis, IN, USA, 7–10 July 2002.
7. Sun, X.; Lu, S. On the mechanisms of flame propagation in methane-air mixtures with concentration gradient. *Energy* **2020**, *202*, 117782. [CrossRef]
8. Sun, X.; Lu, S. Effect of obstacle thickness on the propagation mechanisms of a detonation wave. *Energy* **2020**, *198*, 117186. [CrossRef]
9. Kailasanath, K. Liquid-Fueled detonations in tubes. *J. Propul. Power* **2006**, *22*, 1261–1268. [CrossRef]
10. Wang, Z.W.; Yan, C.J.; Zheng, L.X.; Fan, W. Experimental study of ignition and detonation initiation in two-phase valveless pulse detonation engines. *Combust. Sci. Technol.* **2009**, *181*, 1310–1325. [CrossRef]
11. Wang, Z.W.; Chen, X.G.; Huang, J.J.; Peng, C.X. Semi-free-jet simulated experimental investigation on a valueless pulse detonation engine. *Appl. Therm. Eng.* **2014**, *62*, 407–414. [CrossRef]
12. Wang, Z.W.; Zhang, Y.; Huang, J.J.; Liang, Z.J.; Zheng, L.X.; Lu, J. Ignition method effect on detonation initiation characteristic in a pulse detonation engine. *Appl. Therm. Eng.* **2016**, *93*, 1–7. [CrossRef]
13. Wang, Z.W.; Zhang, Y.; Chen, X.G.; Liang, Z.J.; Zheng, L.X. Investigation of hot jet effect on detonation initiation characteristics. *Combust. Sci. Technol.* **2017**, *189*, 498–519. [CrossRef]
14. Schauer, F.R.; Miser, C.L.; Tucker, K.C. Detonation initiation of hydrocarbon-air mixtures in a pulsed detonation engine. In Proceedings of the 43rd AIAA Aerospace Sciences Meeting and Exhibit, Reno, NV, USA, 10–13 January 2005.
15. Card, J.; Ciccarelli, G. DDT in fuel-air mixtures at elevated temperatures and pressures. *Shock Waves* **2005**, *14*, 167–173. [CrossRef]
16. Brophy, C.M.; Sinicaldi, J.O.; Netzer, D.W.; Johnson, R.G. Operation of a JP10/air pulse detonation engine. In Proceedings of the 36th AlAA/ASME/SAE/ASEE Joint Propulsion Conference, Huntsville, AL, USA, 17–19 July 2000.
17. Akbar, R.; Thibault, P.A. Detonation properties of unsensitized and Sensitized JP-10 and Jet-A fuels in air For pulse detonation engines. In Proceedings of the 36th AlAA/ASME/SAE/ASEE Joint Propulsion Conference, Huntsville, Al, USA, 17–19 July 2000.
18. Helfrich, T.M.; King, P.I.; Hoke, J.L.; Schauer, F.R. Effect of supercritical fuel injection on cycle performance of pulsed detonation engine. *J. Propul. Power* **2007**, *23*, 748–755. [CrossRef]
19. Frolov, S.M. Fast deflagration-to-detonation transition. *Russ. J. Phys. Chem. B* **2008**, *2*, 442–455. [CrossRef]
20. Frolov, S.M.; Aksenov, V.S. Deflagration-to-detonation transition in a kerosene-air mixture. *Dokl. Phys. Chem.* **2007**, *416*, 261–264. [CrossRef]
21. Huang, Y.; Tang, H.; Li, J.; Wang, J. Deflagration-to-detonation transition of kerosene-air mixtures in a small-scale pulse detonation engine. *Proc. Inst. Mech. Eng. Part G J. Aerosp. Eng.* **2011**, *225*, 441–448.
22. Li, J.M.; Teo, C.J.; Chang, P.H.; Li, L.; Lim, K.S.; Khoo, B.C. Excessively fuel-rich conditions for cold starting of liquid-fuel pulse detonation engines. *J. Propul. Power* **2017**, *33*, 71–79. [CrossRef]
23. Li, J.Z.; Wang, J.H.; Fan, Y.X.; Zhang, Y.L.; Zhang, J.Z. Detonation pressure properties of kerosene aero-valve pulse detonation engine. *J. Propuls. Technol.* **2005**, *26*, 443–447. (In Chinese)
24. Xu, P. *Research on Kerosene/Air Pulse Detonation Engine-Effect of Air and Fuel-Injection on Performance*; Nanjing University of Aeronautics and Astronautics: Nanjing, China, 2007. (In Chinese)
25. Nguyen, V.B.; Teo, C.J.; Chang, P.H.; Li, J.M.; Khoo, B.C. Numerical investigation of the liquid-fueled pulse detonation engine for different operating conditions. *Shock Waves* **2019**, *29*, 1205–1225. [CrossRef]
26. Qiu, H.; Su, Z.; Xiong, C. Experimental investigation on multi-cycle two-phase spiral pulse detonation tube of two configurations. *Proc. Inst. Mech. Eng. Part G J. Aerosp. Eng.* **2018**, *233*, 4166–4175. [CrossRef]
27. Lu, J.; Zheng, L.X.; Wang, Z.W.; Chen, X.G. Operating characteristics and propagation of back-pressure waves in a multi-tube two-phase valveless air-breathing pulse detonation combustor. *Exp. Therm. Sci.* **2015**, *61*, 12–23. [CrossRef]
28. Ibrahim, I.A.; Farag, T.M.; Abdel-baky, M.E.; Abd El-samed, A.K.; Gad, H.M. Experimental study of spray combustion characteristics of air-blast atomizer. *Energy Rep.* **2020**, *6*, 209–215. [CrossRef]
29. Wang, Y.; Wang, K.; Fan, W.; He, J.; Zhang, Y.; Zhang, Q.; Yao, K. Experimental study on the wall temperature and heat transfer of a two-phase pulse detonation rocket engine. *Appl. Therm. Eng.* **2017**, *114*, 387–393. [CrossRef]